Bull Earthquake Eng (2016) 14:747–767
DOI 10.1007/s10518-015-9846-7

ORIGINAL RESEARCH PAPER

# Floor response spectra in RC frame structures designed according to Eurocode 8

C. Petrone[1] · G. Magliulo[1] · G. Manfredi[1]

Received: 27 November 2014 / Accepted: 17 November 2015 / Published online: 23 November 2015
© Springer Science+Business Media Dordrecht 2015

**Abstract** Nonstructural components (NSCs) should be subjected to a careful and rational seismic design, in order to reduce the economic loss and to avoid threats to the life safety, as well as what concerns structural elements. The design of NSCs is based on the evaluation of the maximum inertia force, which is related to the floor spectral accelerations. The question arises as to whether Eurocode 8 is able to predict actual floor response spectral accelerations occurring in structures designed according to Eurocode 8. A parametric study is conducted on five RC frame structures in order to evaluate the floor response spectra. The structures, designed according to Eurocode 8, are subjected to a set of earthquakes, compatible with the design response spectrum. Time-history analyses are performed both on elastic and inelastic models of the considered structures. Eurocode formulation for the evaluation of the seismic demand on NSCs does not well fit the numerical results. Some comments on the target spectrum provided by AC 156 for the seismic qualification of NSC are also included.

**Keywords** Floor spectra · Floor acceleration · Nonstructural components · Building codes · Seismic demand

## 1 Introduction

Nonstructural components (NSC) are those systems and components attached to the floors, roof and walls of a building or industrial facility that are not part of the main load-bearing structural system, but may also be subjected to large seismic actions (Villaverde 1997). Recent earthquakes pointed out that NSC damage gives the largest contribution to the

✉ G. Magliulo
gmagliul@unina.it

[1] Department of Structures for Engineering and Architecture, University of Naples Federico II, Via Claudio 21, 80125 Naples, Italy

earthquake economic loss. For instance, damage to cladding panels was the most common damage in precast structures in 2012 Emilia earthquake (Magliulo et al. 2014a). The economic impact could be much more severe if loss of inventory and downtime cost are considered: the cost related to NSCs failure could exceed the replacement cost of the building (Earthquake Engineering Research Institute (EERI) 1984). The performance of NSCs is a key issue in strategic buildings, which must be operative immediately after an earthquake. Moreover, the failure of NSCs may also threaten the life safety. These motivations encouraged several numerical (e.g. Petrovčič and Kilar 2012) and experimental (e.g. Magliulo et al. 2012b; Badillo-Almaraz et al. 2007 among many others) studies on NSCs.

NSCs should be subjected to a careful and rational seismic design, in order to reduce the economic loss and to avoid threats to the life safety, as well as what concerns the structural elements. NSCs are subjected to severe seismic actions, due to the dynamic filtering effect of the ground motion by the primary system, and its impact on the response of the secondary system (Menon and Magenes 2011). The design of NSCs is based on the evaluation of the maximum inertia force, which is related to the floor spectral accelerations. Several research studies were conducted in the past concerning the evaluation of the floor acceleration and the floor response spectra.

Some pioneering papers investigated the seismic response of nonstructural elements anchored or attached to primary structural systems (Sewell et al. 1988; Lin and Mahin 1985; Chen and Soong 1988). Rodriguez et al. (2002) conducted an analytical investigation for the evaluation of the earthquake-induced floor horizontal accelerations in cantilever wall buildings built with rigid diaphragms. The paper describes several methods prescribed by design standards; it proposes a new method for deriving the design horizontal forces. Singh et al. (2006a, b) proposed two methods for calculating the seismic design forces for flexible and rigid NSCs. The validity of such methods was verified by comparing their floor response spectra with the ones obtained for an ensemble of earthquakes exciting several buildings with different numbers of stories. Sankaranarayanan and Medina (2007) evaluated the main factors which influence the floor response spectra in inelastic primary structures. Analyses were carried out on moment-resisting frame structures with 3, 6, 9, 12, 15, and 18 stories. It was found that the most influencing factors are the location of the NSC in the supporting structure, the periods of component and building, the damping ratio of the component, and the level of inelasticity experienced by the supporting structure. An acceleration response modification factor was proposed, which addresses both the decrease and the increase in elastic floor response spectral values due to the yielding of the supporting structure. Wieser et al. (2013) analyzed a set of special moment resisting frame (SMRF) buildings using the incremental dynamic analysis procedure. They proposed an improved estimation for the ratio between peak floor acceleration (PFA) and peak ground acceleration (PGA) by incorporating the elastic natural period of the structure and the expected level of ductility. Moreover, they debated the use of a constant component amplification factor and they proposed an alternative design approach that directly amplifies the ground acceleration spectrum to achieve the desired floor acceleration spectrum.

Few studies (Lucchini et al. 2014) were performed concerning the Eurocode 8 (EC8) (CEN 2004b) formulation for the evaluation of the floor spectral acceleration; according to such floor spectra the seismic demand on a given NSC is evaluated. The available studies did not consider structures designed according to EC8. The question arises as to whether EC8 is able to predict actual floor response spectral accelerations occurring at the design seismic intensity level on EC8-designed structures. Indeed, the structural overstrength due to the Eurocode 8 provisions may significantly influence the floor response spectra.

This research need is the main aim of this study. A set of benchmark RC frame structures are therefore selected and designed according to Eurocode 8. Dynamic nonlinear analyses are performed on the benchmark structures in order to validate the Eurocode formulation; a set of accelerograms compatible with the Eurocode 8 design spectrum is defined. Dynamic analyses are performed both on elastic and inelastic models of the benchmark structures, in order to evaluate the influence of the inelasticity on the definition of the floor response spectrum. The floor response spectra are compared to Eurocode 8 formulation; some considerations on the PFA and the maximum floor spectral acceleration are also given. Finally, some comments on the target spectrum provided by AC 156, for the seismic qualification of NSCs via shake table tests, are also performed and a modification is proposed.

## 2 Methodology

### 2.1 Description of the parametric study

A parametric study is conducted to investigate the seismic demand on a light acceleration-sensitive NSC in multi-story RC frames. 2D frame structures are considered: they are representative of a tridimensional structure with a double symmetric plan and with three frames arranged in each direction (Figs. 1, 2). Benchmark structures with different number of stories are considered: 1-, 2-, 3-, 5- and 10-story buildings, with a 3 m interstory height and two 5 m wide bays.

Benchmark structures are designed according to Eurocode 8 (EC8) (CEN 2004b) provisions. A 0.25 g design ground acceleration $a_g$ is considered. The horizontal elastic response spectrum is defined referring to a 5 % damping ratio and to a 1.2 soil factor, i.e. soil type B. The seismic design meets the ductility class “high” (DCH) requirements: the behavior factor is equal to 4.95 for 10-story building and 5.85 for multi-story frames. The

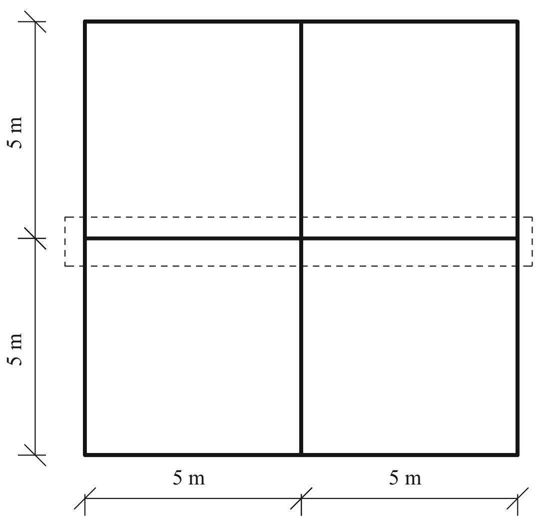


Fig. 1 Plan view of the benchmark structures

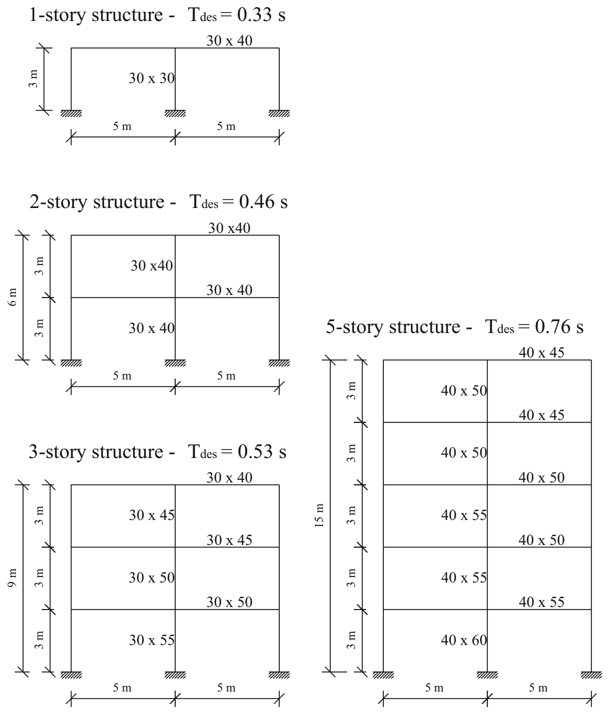


**Fig. 2** Lateral view of the considered building models and their design fundamental period ($T_{des}$). Dimensions of the cross sections are in (cm)

sizing of primary elements is strongly influenced, especially for tall structures, by the restricted value of normalized design axial force, i.e. the ratio between the average compressive stress and the concrete compression strength; this value must not exceed 0.55. Moreover, seismic detailing requirements in terms of longitudinal and transversal reinforcements provide an amount of reinforcement which is larger than strictly required by the design analysis. They induce large structural overstrength which significantly influence the global behavior of the structure, as discussed in Sect. 2.4. A halved moment of inertia is considered for the primary elements during the design phase, according to EC8, in order to take into account the effect of cracking. The fundamental period of the benchmark structures, evaluated according to such a "reduced" flexural stiffness, are listed in Fig. 2.

## 2.2 Modeling

Both elastic and inelastic structural responses are investigated. Dynamic analyses are carried out for a set of seven earthquake records, on both linear and nonlinear models. Rigid diaphragms are considered for each floor; a third of the seismic mass of the corresponding 3D building is assigned to a master joint at each floor. Analyses are performed using the OpenSees program (McKenna and Fenves 2013). The linear modeling provides that the primary elements are modeled as elastic beam-column elements with the gross moment of inertia. Concrete is modelled as an elastic material with a Modulus of Elasticity equal to 31,476 MPa, according to the C25/30 class concrete assumed during the design phase.

A lumped plasticity nonlinear approach is also considered: it is assumed that the primary elements have an elastic behavior and that any inelasticity source is lumped in plastic hinges at their ends. Moment–rotation envelopes in the plastic hinges are defined according to the formulation suggested by Haselton (2006). The nonlinear behavior of the plastic hinges is defined by a peak-oriented hysteretic rule, which simulate the modified Ibarra–Medina–Krawinkler (Ibarra et al. 2005) deterioration model. Cracking point is neglected, i.e. the initial stiffness is equal to the yielding secant stiffness. Appropriate cross sections are defined for each element considering the actual geometry and steel reinforcement in order to determine the moment–curvature diagrams. The cross section is divided into fibers and a stress–strain relationship is defined for each fiber. Different constitutive laws are applied to three different kinds of fibers: unconfined concrete law is associated to cover fibers, confined concrete law is associated to core fibers and steel law is associated to the longitudinal reinforcement fibers. The stress–strain relationship proposed by Mander et al. (1988) is used both for unconfined and confined concrete. The B450C steel class is adopted with a bilinear with hardening relationship. The steel mechanical characteristics are calculated according to Eurocode 2 (Table C.1, "Properties of reinforcement") (CEN 2004a).

Table 1 shows the comparison of the first and second vibrational periods of each structure; they can be obtained with either the design-approximated stiffness assumption ($T_{i,des}$) or gross section elastic stiffness ($T_{i,el}$) or inelastic yielding secant stiffness ($T_{i,nl}$). The period range in Table 1 highlights the large uncertainty in the assessment of the structural period during the design phase. This range would have been even wider if the infill contribution to the lateral stiffness had been considered. It is particularly valid in case of brick infills, widespread in the European area (Petrone et al. 2014; Asteris and Cotsovos 2012).

## 2.3 Ground motion records

The structural response is investigated through time history analyses. Therefore, a suitable set of 7 accelerograms (Table 2) is provided, matching the design spectrum at the life safety limit state, i.e. 475 years return period earthquake, according to the EC8 recommendations (Maddaloni et al. 2012):

- the mean of zero-period spectral response acceleration values, which is equal to 3.69 $m/s^2$, is larger than the design value, i.e. $a_g \cdot S$;
- the mean elastic spectrum of the selected ground motions is larger than 90 % of the design elastic response spectrum in the range of periods between $0.2T_{1,min}$ and $2T_{1,max}$. $T_{1,min}$ and $T_{1,max}$ are, respectively, the minimum and the maximum fundamental period of the benchmark 2D structures (Fig. 3).

**Table 1** Comparison of the first and second vibrational periods evaluated according to different models of the considered structures

| No. story (−) | $T_{1,des}$ (s) | $T_{1,el}$ (s) | $T_{1,nl}$ (s) | $T_{2,el}$ (s) | $T_{2,nl}$ (s) |
|---|---|---|---|---|---|
| 1 | 0.33 | 0.23 | 0.42 | – | – |
| 2 | 0.46 | 0.32 | 0.64 | 0.11 | 0.22 |
| 3 | 0.53 | 0.37 | 0.78 | 0.14 | 0.26 |
| 5 | 0.76 | 0.52 | 1.11 | 0.18 | 0.37 |
| 10 | 1.39 | 0.95 | 2.12 | 0.36 | 0.78 |

**Table 2** Waveform ID, earthquake ID (Eqk ID) and name, date, moment magnitude ($M_W$), epicentral distance (R), horizontal direction (Dir.) and peak ground acceleration (PGA) of the accelerograms selected for dynamic analyses (Ambraseys et al. 2002)

| Waveform | Eqk ID | Earthquake name | Date | $M_W$ (−) | R (km) | Dir. | PGA (m/s$^2$) |
|---|---|---|---|---|---|---|---|
| 146 | 65 | Friuli (aftershock) | 15/09/1976 | 6.0 | 14 | y | 3.296 |
| 197 | 93 | Montenegro | 15/04/1979 | 6.9 | 24 | x | 2.880 |
| 413 | 192 | Kalamata | 13/09/1986 | 5.9 | 10 | y | 2.910 |
| 414 | 192 | Kalamata | 13/09/1986 | 5.9 | 11 | x | 2.354 |
| 414 | 192 | Kalamata | 13/09/1986 | 5.9 | 11 | y | 2.670 |
| 4673 | 1635 | South Iceland | 17/06/2000 | 6.5 | 15 | y | 4.677 |
| 6334 | 2142 | South Iceland (aftershock) | 21/06/2000 | 6.4 | 11 | y | 7.070 |

It is underlined that the use of a small amount of accelerograms may cause large standard errors of estimation of floor response spectra (Shome et al. 1998), since the standard error of estimation is approximately the sample dispersion divided by $\sqrt{N}$, where $N$ is the sample size.

## 2.4 Preliminary nonlinear static analyses

The acceleration demand on NSCs depends on both the dynamic interaction with the primary structure and the structural energy dissipation (Rodriguez et al. 2002; Politopoulos 2010). The energy dissipation tends to reduce the intensity of the acceleration time history at a given floor. Structural overstrength, instead, lets the structure dissipate less energy and reduce the ductility demand compared to the ductility assumed during the design phase. The smaller the ductility demand is, the larger the floor accelerations are: the latter tend to the floor accelerations evaluated on the elastic structure (Medina et al. 2006).

In order to estimate the effective structural response and evaluate the overstrength ratios, nonlinear static analyses are performed applying a pattern of lateral forces proportional to the first mode displacement shape. Indeed, nonlinear static analyses may give

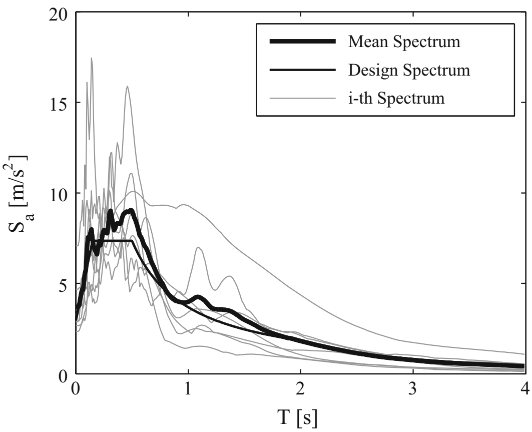


**Fig. 3** Comparison between the mean acceleration response spectrum of the adopted set of accelerograms and the design spectrum according to EC8

an accurate prediction of the seismic demand estimated according to nonlinear dynamic analyses (D'Ambrisi et al. 2009). For each structure, the relationship between the base shear force and the roof displacement is determined. The pushover curve, evaluated on the MDOF system, is converted into the capacity curve for the equivalent SDOF system; the idealized bilinear force–displacement relationships are obtained in accordance to the Italian Building Code (Consiglio Superiore dei Lavori Pubblici 2009) (Fig. 4): the ultimate displacement $d_u$ is the SDOF displacement corresponding to a strength reduction equal to the 15 %; the bilinear curve initial stiffness and yielding shear force are obtained imposing that (a) the first branch intersects the capacity curve at 0.6 $F_u$ and (b) the equality of the areas under the actual and the bilinear curves until the ultimate displacement $d_u$.

The bilinear curve can be plotted in the Acceleration-Displacement Response Spectrum (ADRS) plane, where the design spectrum is plotted. In order to investigate the different sources of overstrength, for each structure the following ratios are evaluated (Fig. 5):

- α, the ratio between the spectral acceleration evaluated for the equivalent SDOF structure with a linear behavior ($S_{ae}$) and the spectral acceleration corresponding to the yielding of the SDOF system ($S_{ay}$). This ratio expresses the reduction of the spectral acceleration demand due to the non-linear behavior of the structure; it therefore provides an estimation of the global ductility demand;
- β, the ratio between the spectral acceleration corresponding to the yielding of the SDOF system ($S_{ay}$) and the spectral acceleration that produces the first plastic hinge yielding ($S_{ah}$). This ratio takes into account the overstrength caused by the structural redundancy;
- γ, the ratio between the spectral acceleration corresponding to the first plastic hinge ($S_{ah}$) and the design spectral acceleration ($S_{ad}$). This ratio represents the overstrength due to material properties and design details;
- δ, the ratio between the spectral acceleration demand considered during the design phase ($S_{ae,des}$) and the spectral acceleration evaluated for the equivalent SDOF structure with a linear behavior ($S_{ae}$). This ratio takes into account the reduction of the stiffness in the nonlinear model.

In Fig. 6 the bi-linearized capacity curves of the different structures are plotted in the ADRS plane and compared to the EC8 design spectrum. Yielding of the first plastic hinge is denoted with a circle. Overstrength ratios are listed in Table 3 for the different

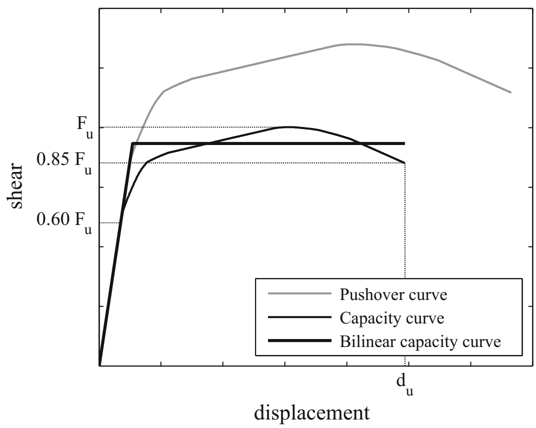


**Fig. 4** Evaluation of the bilinear capacity curve according to the Italian Building Code (Consiglio Superiore dei Lavori Pubblici 2009)

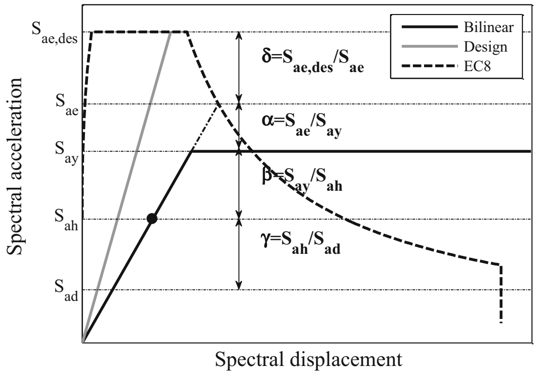


**Fig. 5** Overstrength ratios definition

structures. It shows that RC frames, designed according to Eurocode 8 rules, are characterized by a high global overstrength. A low ductility demand is expected at the design seismic level; the ductility demand is therefore much smaller than the assumed behavior factor q; the effective floor acceleration are not likely to be significantly reduced with respect to the floor accelerations evaluated with the elastic model (Politopoulos 2010).

Moreover, the safety assessment of the structures shows that the displacement capacity is much larger than the demand in RC frame structures designed according to Eurocode 8; the displacement capacity values are omitted for the sake of brevity. Based on the conclusions included in (Magliulo et al. 2007), the safety assessment in the dynamic analysis could be even more conservative.

For all the structures, $\gamma$ values are generally overestimated in this study, due to the adopted plastic hinge model with initial stiffness equal to the yielding secant stiffness. Indeed, the absence of the cracking point in the moment–rotation relationship reduces the bending moment at beam ends due to vertical loads. A larger base shear is then required to reach the yielding in the beam plastic hinges. It should be noted that the assessment of the

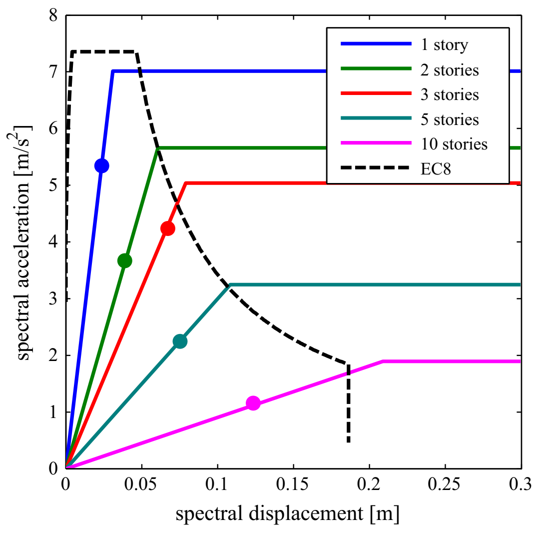


**Fig. 6** Capacity curves of the benchmark structures plotted in the Acceleration Displacement Response Spectrum plane

**Table 3** Overstrength ratios values for the analyzed structures

| No. story | α | β | γ | δ |
|---|---|---|---|---|
| 1 | 1.05 | 1.31 | 3.59 | 1.00 |
| 2 | 1.00 | 1.55 | 2.91 | 1.30 |
| 3 | 0.92 | 1.19 | 3.50 | 1.52 |
| 5 | 1.03 | 1.45 | 2.67 | 1.47 |
| 10 | 0.88 | 1.66 | 2.46 | 1.63 |

total overstrength value, i.e. β times γ, is not much affected by such an approximation and can be considered correctly evaluated.

# 3 Results and discussion

## 3.1 Elastic and inelastic floor response spectra

Dynamic analyses are performed on both elastic and inelastic models; the horizontal acceleration time-histories at different levels are recorded for each selected accelerogram. Floor response spectra are obtained for each floor accelerogram with a 5 % damping ratio; a mean response spectrum is plotted for each floor of the considered structures (Fig. 7). These spectra provide the acceleration demand on NSCs which are connected to the floor and exhibit a fundamental period T. Figure 7 shows the mean floor response spectra, evaluated on both the elastic (dotted line) and inelastic (solid lines) models for the 5-story structure.

Due to the dynamic filtering effect, the primary structure modifies the frequency content of the earthquake; floor accelerogram, amplified with respect to the base accelerogram, has a large frequency content for periods close to the vibration periods of the elastic model. If

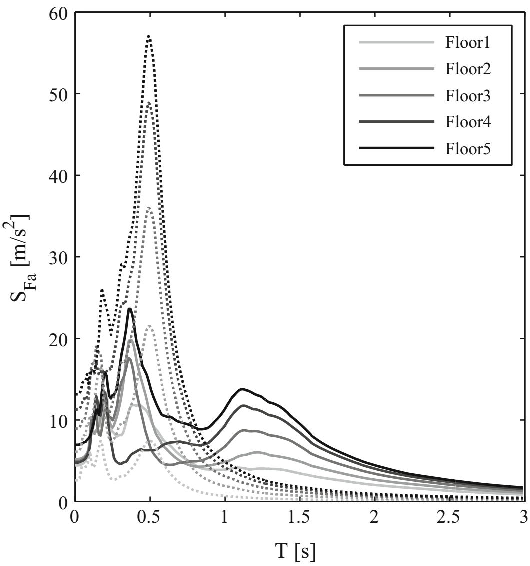


**Fig. 7** Floor response spectra of the 5-story structure evaluated on both the elastic (*dotted line*) and inelastic models (*solid line*)

the NSC period corresponds to one of the natural periods of the structure, a double-resonance phenomenon occurs; floor response spectra exhibit peaks which may exceed five times the acceleration of gravity, i.e. about 20 times the base acceleration, at the top floor of the structure. Two main peaks are recorded corresponding to periods, i.e. $T_{1,el\text{-}eff}$ and $T_{2,el\text{-}eff}$, very close to the periods associated to the first and second vibration modes, i.e. $T_{1,el}$ and $T_{2,el}$ (Table 1).

Table 4 shows the ratio between the two peak values obtained for the top floor of the different structures ($S_{Fa}(T_{1,el\text{-}eff})/S_{Fa}(T_{2,el\text{-}eff})$). For each floor, the acceleration corresponding to the fundamental period ($T_{1,el\text{-}eff}$) is larger than the one associated to the period of second mode ($T_{2,el\text{-}eff}$), except for the 10-story structure. As expected, the influence of the higher modes on the definition of the floor spectra is predominant for such a tall building.

Inelastic floor response spectra (solid lines in Fig. 7), show that the curves exhibit peaks at periods, i.e. $T_{1,nl\text{-}eff}$ and $T_{2,nl\text{-}eff}$, much larger than the elastic ones, due to the different initial stiffness of the two models (see Sect. 2.2). Figure 8 shows the comparison between elastic and inelastic floor response spectra for the remaining structures. The following comments can be drawn:

- a significant period elongation is exhibited, comparing the peak related to the first structural mode of the elastic model with the inelastic one;
- the comparison of the peak related to the first structural mode of the elastic model with the inelastic one also shows a substantial reduction of the peak spectral ordinate: the maximum spectral values of the inelastic model are less than 3 g for the different structures. The reduction is caused by both the period elongation phenomenon and the ductility demand experienced by the structure. This phenomenon is not observed for the 1-story structure, because the period elongation does not modify the base response spectral ordinate, as denoted by the $\delta$ factor in Table 3;
- higher mode effects are significant in the 10-story structure. Moreover, the peak spectral values associated with the higher modes are slightly reduced in the inelastic model. At lower stories, the spectral values associated with higher modes can be even larger than the elastic ones, as also pointed out by Chaudhuri and Villaverde (2008) in a research study on steel moment-resisting frames. This phenomenon confirms that the higher mode influence becomes more significant in the inelastic range (Fischinger et al. 2011; Rejec et al. 2012).

**Table 4** Ratio between the first two peak floor spectral accelerations obtained for the top floor of the different structures in both the elastic and in inelastic models

| No. story (–) | $S_{Fa}(T_{1,el\text{-}eff})/S_{Fa}(T_{2,el\text{-}eff})$ (–) | $S_{Fa}(T_{1,nl\text{-}eff})/S_{Fa}(T_{2,nl\text{-}eff})$ (–) | $S_{Fa,max\ el}/S_{Fa,max\ nl}$ (–) |
|---|---|---|---|
| 1 | – | – | 1.11 |
| 2 | 3.79 | 1.52 | 2.43 |
| 3 | 1.90 | 0.94 | 1.90 |
| 5 | 2.18 | 0.58 | 2.42 |
| 10 | 0.68 | 0.39 | 1.17 |

Comparison between maximum floor spectrum acceleration in the elastic and inelastic models

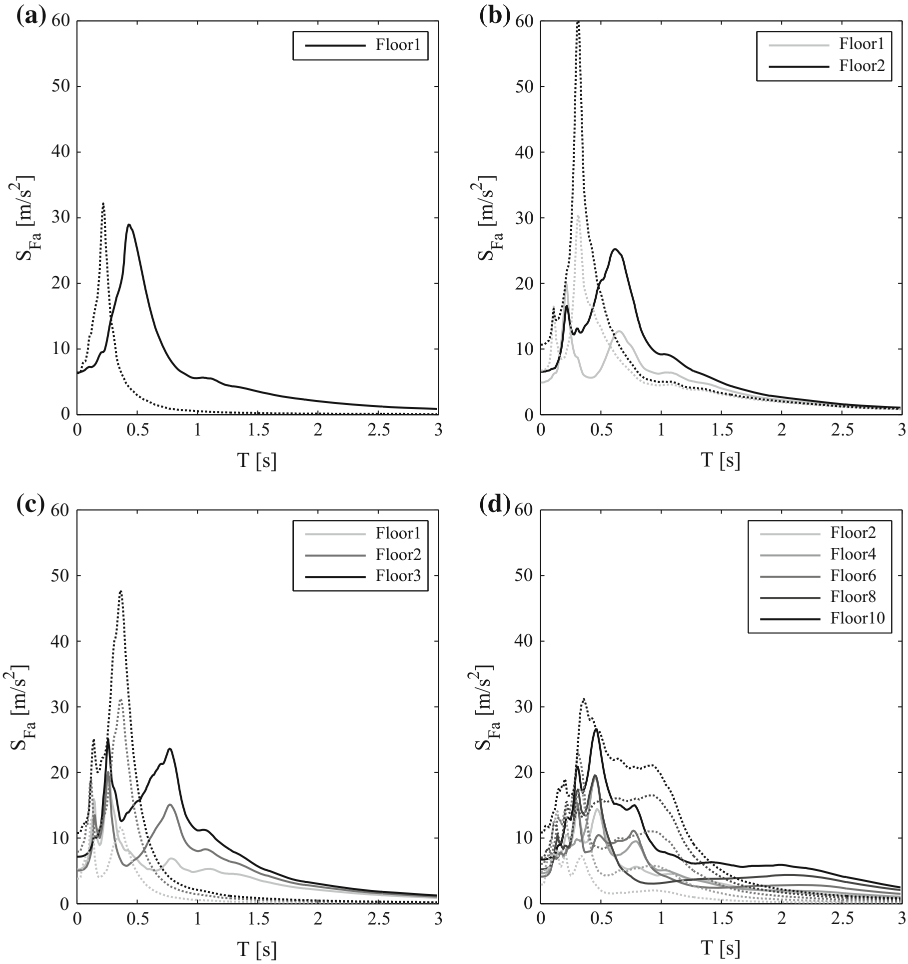


**Fig. 8** Floor response spectra of the **a** 1-story, **b** 2-story, **c** 3-story and **d** 10-story structures evaluated on both the elastic (*dotted line*) and inelastic models (*solid line*)

Table 4 shows the ratio between the two floor spectral peak values for the top floor of the different structures in the inelastic models ($S_{Fa}(T_{1,nl\text{-}eff})/S_{Fa}(T_{2,nl\text{-}eff})$); the ratio between the maximum elastic and inelastic spectral ordinate is also listed ($S_{Fa,max\ el}/S_{Fa,max\ nl}$). It can be observed that the inelastic spectral acceleration reduction is significantly far from the assumed behavior factor, due to the large structural overstrength (see Sect. 2.4). It is also confirmed that the energy dissipation is mostly related to the first mode; indeed the peak value associated to $T_{2,nl\text{-}eff}$ may exceed the peak value associated to $T_{1,nl\text{-}eff}$. It can be concluded that in case inelastic models are considered, higher modes give a larger contribution to the definition of the floor spectral ordinates.

From these considerations it follows that three factors mainly influence the floor spectral acceleration caused by the earthquakes compatible with the design spectrum (Sankaranarayanan and Medina 2007): (1) the structural ductility demand level, strongly related to the structural overstrength; (2) the relative structural height where the component is installed; (3) the dynamic characteristics of NSCs in terms of natural period, normalized with respect to the structural period.

### 3.2 Floor amplification evaluation

The ratio between PFA and PGA is plotted versus the relative height in Fig. 9 for the benchmark structures, in order to study the floor acceleration magnification with height. The PFA over PGA trend with the relative structural height is shown for both elastic and inelastic models.

The elastic model diagrams, which represent the average response of each structure, show an almost linear trend and they reach values of PFA/PGA close to 3.0 at the top floor. At the same relative height, the values of the ratio PFA/PGA are larger for structures with a larger number of floors, except for the tallest structure. At the lower stories of tall structures, PFA values are smaller than PGA values.

Inelastic models also show a linear trend. In this case the amplification is smaller than in elastic models: the PFA/PGA values are always greater than one and they reach the maximum value, close to 2, at the top story. As pointed out by Wieser et al. (2013) and Ray-Chaudhuri and Hutchinson (2011), the yielding of the structure and the period elongation cause a significant reduction of PFAs.

Many literature research papers, e.g. Taghavi and Miranda (2005) and Rodriguez et al. (2002) among many others, highlighted a whiplash effect in the topmost floor of tall structures; this phenomenon is caused by the large contribution of the higher modes to the PFAs in the top stories. The results presented in this paper (Fig. 9) also highlight such a phenomenon, especially for the 10-storey frame. However, the whiplash effect is less conspicuous than in reference studies. The low ductility demand experienced by the structures considered in the present study could have caused this phenomenon. Indeed,

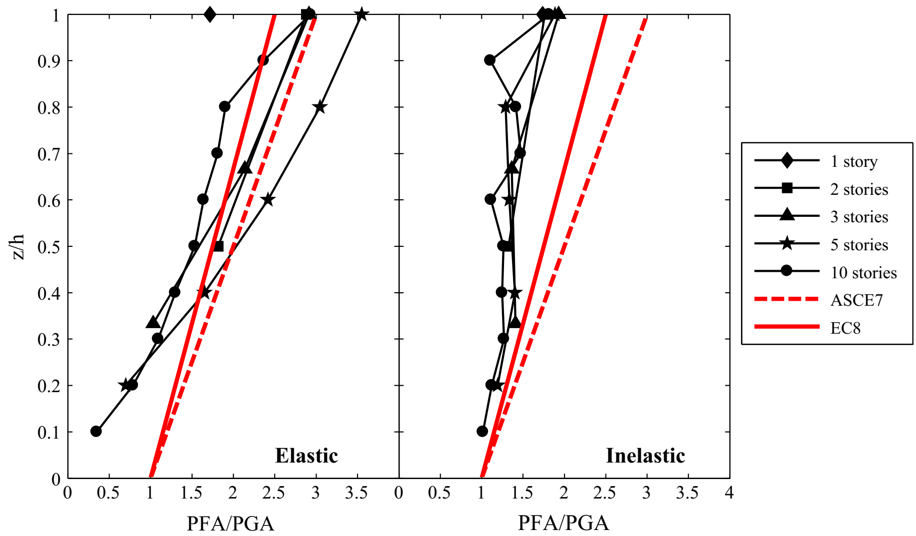


**Fig. 9** Ratio between peak floor acceleration and peak ground acceleration, versus the relative height ($z/h$) for the different considered structures compared to the provisions included in ASCE7 and EC8

higher modes influence becomes more significant in the inelastic range (Fischinger et al. 2011; Rejec et al. 2012).

Both the elastic and inelastic trends are compared to ASCE7 (American Society of Civil Engineers 2010) and Eurocode 8 provisions (Fig. 9). The ASCE7 and EC8 provisions are described respectively in Sect. 3.5 and 3.4. Such a comparison shows that both the ASCE7 and EC8 provisions are safe-sided for the inelastic diagrams, which are the most realistic ones. The New Zealand building code (NZS 1170.5) (Council of Standards New Zealand 2004) provides a linear PFA/PGA envelope with the height, from a unit value at the base to three at the top, for structures up to 12 m high; for taller structures a constant three amplification value is provided from 12 m height to the top of the structure. This trend would also overestimate the analysis results (Fig. 9). Finally, a linear trend that goes from one at the base to two at the top would better fit the outcomes of the nonlinear analyses.

### 3.3 Component amplification evaluation

The ratio between the maximum floor spectral acceleration and the PFA, i.e. $a_p$, is plotted versus the relative floor height for each floor of the analyzed structures in order to study the floor acceleration magnification on the component (Fig. 10). This ratio represents the amplification of the floor acceleration demand for a NSC that is in tune with the primary structure.

The inelastic floor magnifications on NSCs are slightly smaller than the elastic ones. For the 10-story structure, the inelastic $a_p$ values are larger than the elastic ones. This is due to the fact that the largest spectral ordinate value is given by higher modes, which are only slightly influenced by the nonlinearity experienced by the structure (Fig. 8d) (Fischinger et al. 2011; Rejec et al. 2012); the PFA values, instead, are influenced by the first mode; they significantly decrease in the inelastic model (Fig. 9). Hence, the ratio between the maximum floor spectral acceleration and the PFA could be larger in inelastic models in tall structures.

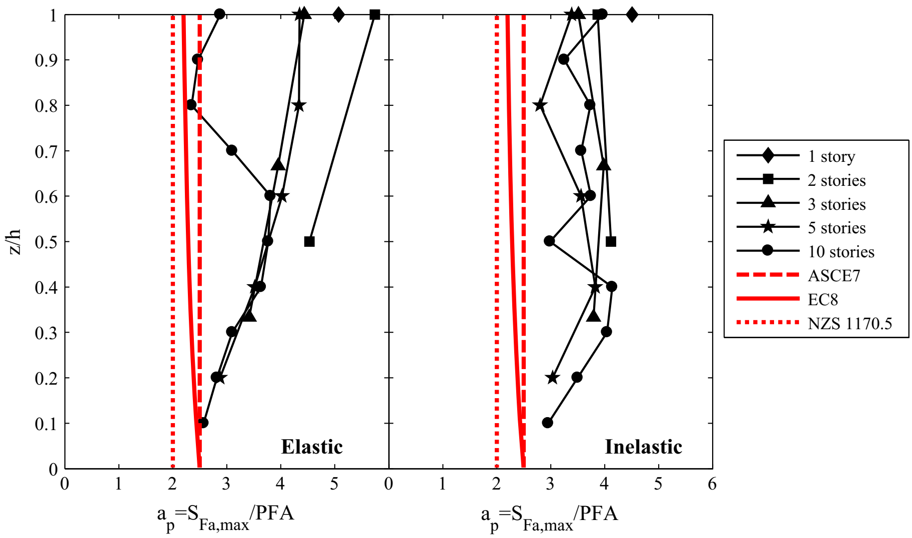


**Fig. 10** Floor acceleration magnification on nonstructural components

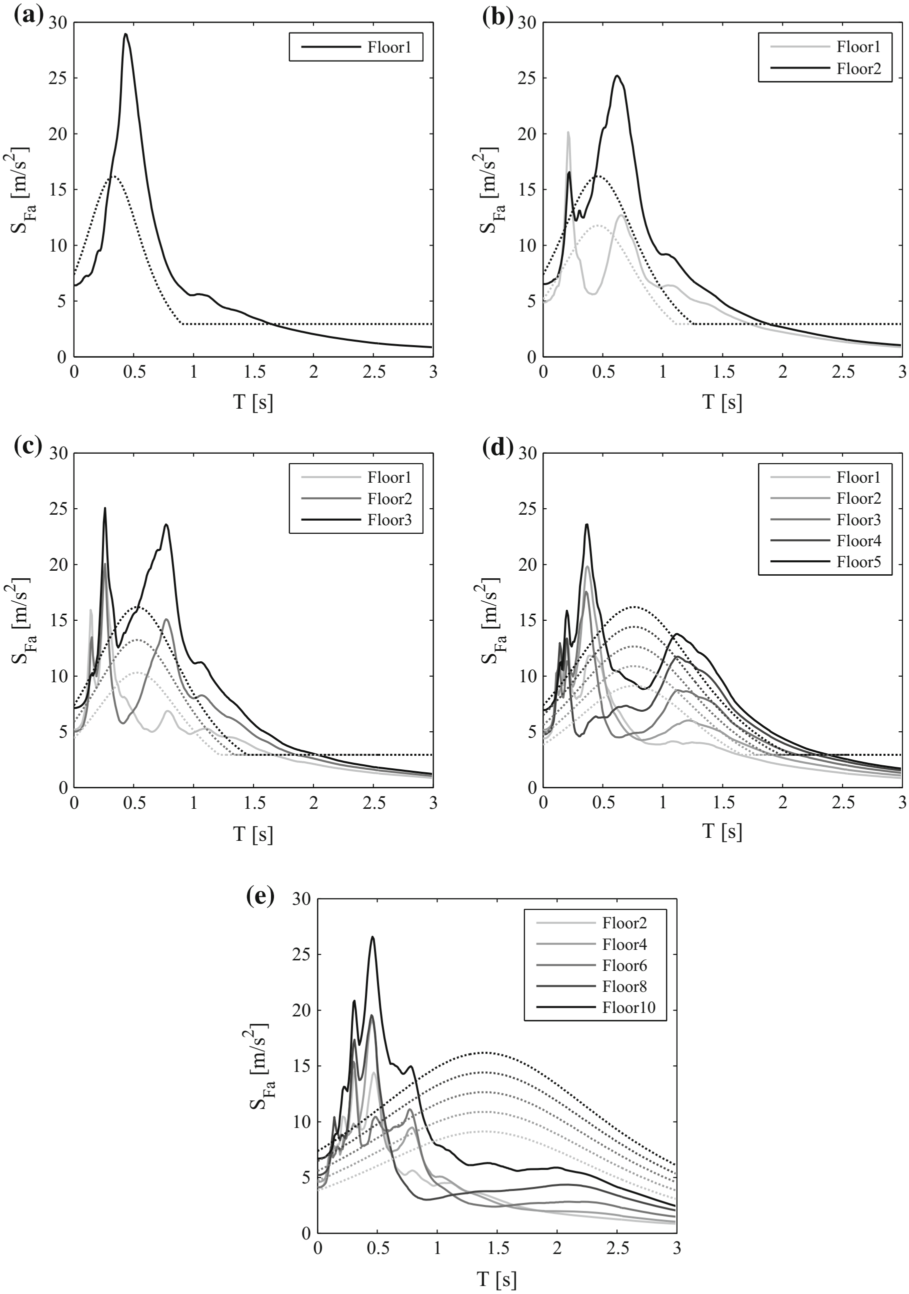


**Fig. 11** Comparison between effective inelastic floor response spectra (*solid lines*) and floor response spectra evaluated according to Eurocode 8 (*dashed lines*) for the **a** 1-story, **b** 2-story, **c** 3-story, **d** 5-story and **e** 10-story structures

Assuming both elastic and inelastic models, the trend is almost constant with the height and the $a_p$ values are greater than the values recommended by ASCE7, NZS 1170.5 and EC8 (see Sects. 3.5 and 3.4, respectively, for ASCE 7 and EC8 provisions). A significant underestimation of the $a_p$ values in the current building codes is pointed out, confirming the results included in (Medina et al. 2006).

### 3.4 Comparison with EC8 formula and limitations

In order to take into account the realistic behavior of the primary structures, inelastic floor spectra should be considered. These curves are compared with Eurocode 8 formulation (CEN 2004b) for the evaluation of the floor response spectrum acceleration $S_a$ acting on a NSC:

$$S_a = \alpha \cdot S \cdot \left[ \frac{3 \cdot (1 + z/H)}{1 + (1 - T_a/T_1)^2} - 0.5 \right] \cdot g \geq \alpha \cdot S \cdot g \tag{1}$$

where $\alpha$ is the ratio between the ground acceleration and the gravity acceleration g, S is a soil amplification factor, z/H is the relative structural height at which the component is installed, $T_a$ is the NSC period, $T_1$ is the fundamental period of the primary structure, assumed during the design phase.

The design floor response spectrum is influenced by the ratio between the NSC period and the structural period, as well as by the level at which the NSC is installed. The formulation does not clearly distinguish the different factors which affect the floor spectral accelerations; a different approach is provided, instead, by ASCE7 formulation (American Society of Civil Engineers 2010) (see Sect. 3.5). However, EC8 formulation implicitly assumes that the PFA linearly ranges from PGA at the base to 2.5 times PGA at the top of the structure, whereas $a_p$ linearly ranges from 2.5 at the base to 2.2 at the top of the structure, as already mentioned in Sect. 3.2 and 3.3. Moreover, the maximum $S_a$ value is equal to 5.5 times the PGA, i.e. the spectral acceleration acting on a component placed at the top floor which is in tune with the structure.

For different values of $T_a$ and for each floor, the Eurocode formulation provides a curve that shows the maximum value for $T_a$ equal to $T_1$. In Fig. 11 both inelastic floor spectra and design Eurocode 8 floor spectra are plotted for the benchmark structures. The Eurocode formulation underestimates the maximum floor acceleration demand for a wide range of NSC periods, whereas it overestimates the acceleration demand on NSCs with a period close to the design period of the structure ($T_{des}$ in Fig. 2). Moreover the peak of the Eurocode curve is reached at the design period, which is smaller than the effective one for all the inelastic models (Table 1).

Eurocode formulation does not take into account higher modes: a significant underestimation is recorded in the range of periods close to the higher modes periods of vibration. The effective floor spectrum acceleration can be significantly underestimated, especially for tall structures, e.g. the 10-story structure in Fig. 11e, where higher modes are predominant.

The approach proposed by Fathali and Lizundia (2011), who considered a constant floor response spectral acceleration in a wide range of periods, could be adopted. It would allow removing both the issue related to the uncertainty in the definition of the structural fundamental period and the non-inclusion of the higher mode effects in the floor response spectra.

The effect of the higher modes in the floor response spectra is influenced by the nonlinear excursion that the structure experiences during the earthquake motion (see Sect. 3.1). Both European and US codes do not explicitly take into account the reduction of the floor response spectra due to the nonlinear behavior of structures; however, the adoption of a low $a_p$ value, i.e. from 2.2 to 2.5, could include the reduction due to the nonlinear behavior of the main structure. The $a_p$ values recorded in structures which experience large ductility demand are typically smaller than the ones recorded in Fig. 10, due to the low level of ductility demand experienced by the benchmark structures.

It would be preferable to explicitly include the ductility demand level in code formulas for the evaluation of floor spectra, as mentioned in (Medina et al. 2006). The ductility level experienced by a structure, subjected to the design earthquake motion, is strongly influenced by the structural overstrength, which is in turn related to the prescriptions included in the code itself (see Sect. 2.1). Hence, the definition of a formula that includes the structural ductility demand level would certainly be code-dependent.

The structural overstrength of a given building cannot be easily assessed during the design phase. Moreover, it is related to many factors, e.g. the bay width, the presence of irregularities in plan or elevation and the design PGA among others, which are not considered in this research study. Hence, a very wide parametric study is required to define a code formula that explicitly takes into account the ductility level that the structure experiences.

Alternatively, the code formulation for the evaluation of the NSC demand could be referred to the elastic floor response spectrum. This approach would be too conservative, i.e. acceleration on components could be up to 20 times the acceleration at the base (see Sect. 3.1); moreover, it would not reflect the realistic behavior of the structure in terms of both the fundamental period and the ability of the structure to dissipate energy.

Finally, it is concluded that Eurocode could not adequately address the seismic demand on acceleration-sensitive NSCs, as pointed out by Velasquez et al. (2012) from the analysis of floor time-history accelerations recorded during a shake-table test campaign.

### 3.5 Comparison with AC156 target spectrum

AC156 (International Conference of Building Officials (ICBO) 2000) provides a procedure for the seismic qualification of NSCs by shake table testing. The protocol provides that NSCs are shaken with a horizontal accelerogram whose response spectrum (Test Response Spectrum) is compatible with the Required Response Spectrum (RRS) shown in Fig. 12.

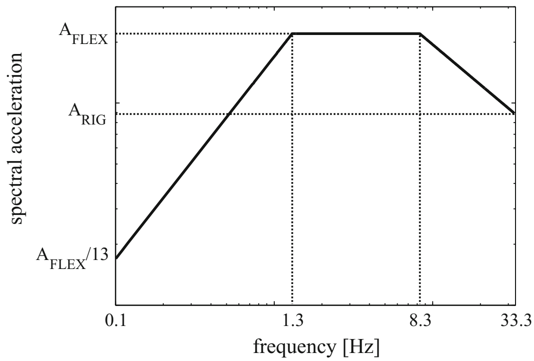


**Fig. 12** AC156 horizontal Required Response Spectrum (RRS) for qualification testing of nonstructural components

The RRS reflects the provisions included in ASCE7 (American Society of Civil Engineers 2010) for the seismic demand evaluation on NSCs. According to ASCE7, NSCs are designed in order to withstand a force $F_p$ acting in their centroid, evaluated as follows:

$$F_p = \frac{0.4 \cdot a_p \cdot S_{DS} \cdot W_p}{\left(\frac{R_p}{I_p}\right)} \cdot \left(1 + 2 \cdot \frac{z}{h}\right) \tag{2}$$

where $a_p$ is the floor-to-component amplification factor, $S_{DS}$ is the design spectral acceleration at short periods, $W_p$ is the weight of the component, $R_p$ is the component force reduction factor, $I_p$ is the importance factor and z/h is the relative height ratio where the component is installed. The force $F_p$ is limited to be not larger than 1.6 times $S_{DS} \cdot I_p \cdot W_p$.

The AC156 RRS must be matched in the frequency range between 1.3 and 33.3 Hz; it is defined by the following values:

$$A_{FLEX} = S_{DS} \cdot \left(1 + 2 \cdot \frac{z}{h}\right) \tag{3}$$

$$A_{RIG} = 0.4 \cdot S_{DS} \cdot \left(1 + 2 \cdot \frac{z}{h}\right) \tag{4}$$

AC156 assumes that $R_p/I_p$ is equal to 1, since during the seismic simulation test, the specimen "will respond to the excitation and inelastic behavior will naturally occur"; the factor $a_p$ is set equal to 2.5 for flexible components (1.3 Hz < f < 8.3 Hz) and 1 for rigid components (f > 8.3 Hz). $A_{FLEX}$ is limited to a maximum value of 1.6 times $S_{DS}$.

For NSCs commonly installed at different stories of a structure, the ratio z/h is usually set equal to 1, i.e. considering the most intense condition. Many applications of the AC156 protocol can be found in literature (Magliulo et al. 2012a, b, 2014b; Petrone et al. 2014; Badillo-Almaraz et al. 2007).

The spectrum provided by AC156 is aimed at inducing the maximum seismic demand acting on a given NSC, whatever the structural typology is. Therefore, it can be interpreted as an envelope of all the possible floor response spectra that are recorded at a given z/h

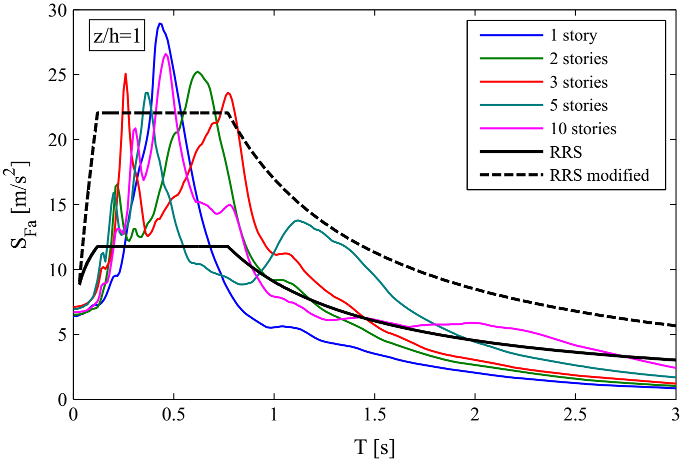


**Fig. 13** AC156 Required Response Spectrum (RRS), original and proposed, compared to the floor response spectrum at the top story of the different structures

ratio of a generic building typology. For this reason the AC156 RRS, evaluated for z/h ratio equal to 1, is compared to the floor response spectra recorded at the top story of the benchmark structures (Fig. 13). $S_{DS}$ is evaluated as 2.5 times the design PGA of the analyzed structures, as reported in ASCE7. The comparison underlines the significant underestimation of the floor spectrum ordinates in AC156 RRS. For low period components, instead, AC156 RRS gives larger accelerations, consequently to the comparison shown in Fig. 9.

The above mentioned $A_{FLEX}$ upper bound limitation, i.e. $1.6 \cdot S_{DS}$, reflects the similar limitation that ASCE7 defines on the force $F_p$ acting on the component. However, the limitation on the force $F_p$ should not be extended to the RRS, since the RRS does not include the reduction caused by the inelastic behavior of the tested NSC, i.e. the $R_p$ factor. In other words, the limitation on the force acting on the component implicitly assumes that a minimum $R_p$ value is considered (ASCE7 provides $R_p$ values larger than 1.5 for the different considered NSCs). Conversely, the seismic qualification testing does not include such a reduction. Medina (2013) also proposed to consider the removal of the upper limit of the force $F_p$, based on structural analyses on 3- 9- and 15-story structural wall systems. If the limitation on $A_{FLEX}$ is removed, the RRS (dotted line in Fig. 13) will better match the floor response spectra resulting from the analyses. In such a case, the RRS can be interpreted as an envelope of all the possible floor response spectra which can be recorded at a given z/h ratio of a generic building. The upper bound limitation on $A_{FLEX}$ also vanishes the influence of the normalized height *z/h* on the RRS (Fig. 14a) for the top floors of a structure; for instance, the RRS for the 5-story structure at the different levels are equal, except for the first floor. The influence of the z/h ratio is fully considered in case the limitation on $A_{FLEX}$ is removed (Fig. 14b).

The above mentioned considerations could lead to a misinterpretation of past shake table tests performed according to AC156. Indeed, a given SDS value would induce a larger seismic demand on the tested NSC if the limitation on $A_{FLEX}$ is removed. It is underlined that the comparison refers to a limited number of RC frame structures. A larger set of buildings is required in order to generalize such a conclusion.

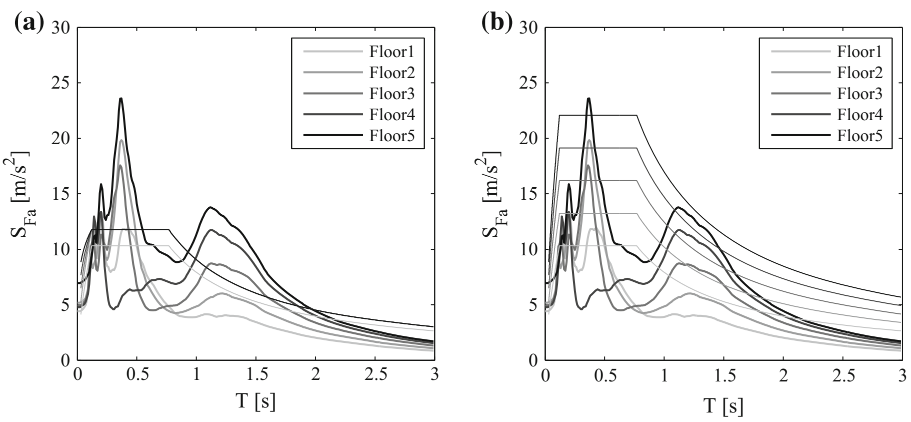


**Fig. 14** AC156 Required Response Spectrum (*thin lines*), **a** original and **b** proposed, compared to the floor response spectra of the 5-story structure (*thick lines*)

## 4 Conclusions

A parametric study for the assessment of the accuracy of the Eurocode 8 formulation for the floor response spectra in RC frame structures, i.e. 1- 2- 3- 5- and 10-story structures, is conducted. The structures, designed according to Eurocode 8, are subjected to a set of earthquakes that are compatible with the design response spectrum. Preliminary nonlinear static analyses show that the benchmark structures are characterized by a significant overstrength, due to some geometric limitations included in the Eurocode 8.

Time-history analyses are performed both on elastic and inelastic models of the benchmark structures. The comparison between elastic and inelastic floor response spectra indicates a substantial reduction of the peak spectral ordinate associated to the first mode; moreover, the peak occurs at a longer period, due to the period elongation phenomenon. The peak spectral values associated with the higher modes are only slightly reduced in the inelastic model. At lower stories, the spectral values associated to higher modes can be even larger than the elastic ones.

The ratio between PFA and PGA trend with the relative structural height shows that ASCE7, NZS 1170.5 and EC8 provisions are safe-sided. A linear trend that goes form 1 at the base of the structure to 2 at the top would better fit the outcomes of the analyses. The yielding of the structure gives a significant contribution to the PFA reduction. The component amplification, i.e. the ratio between the maximum floor spectral value and the PFA, is almost constant with the height for both elastic and inelastic models. An unsafe-sided estimation of the $a_p$ values in the actual building codes is pointed out: the component amplification $a_p$ values are significantly greater than 2.5, which is the value recommended by ASCE7 and EC8, and close to 4.5.

It is found that the Eurocode formulation for the evaluation of the seismic demand on NSCs does not fit well the analysis results in RC frame structures designed according to EC8. It underestimates the maximum floor acceleration demand for a wide range of NSC periods, whereas it overestimates the acceleration demand on NSCs with a period close to the design period of the structure. The underestimation is significant for NSC periods close to the higher modes structural periods, since Eurocode formulation does not include higher mode effects. The urgent need to include the structural ductility demand in code formulas for the evaluation of floor spectra is claimed. However, it is underlined that the ductility level is influenced by the structural overstrength, which is in turn related to the prescriptions included in the reference building code. Hence, the definition of a formula that includes the structural ductility demand level would certainly be code-dependent.

Some comments on the target spectrum provided by AC 156 for the seismic qualification of NSC are included. In particular, it is shown that in case the upper bound limitation on the Required Response Spectrum (RRS) is removed, the RRS well matches the floor response spectra resulting from the analyses on the benchmark structures.

It should be underlined that the above presented results and conclusions are related and limited to a set of five RC "simple" structures designed according to Eurocode 8 for a given seismic intensity level. A very wide parametric study is encouraged in order to define a code formula that explicitly takes into account the ductility level or the structural overstrength. A wide parametric study is needed in order to generalize the results and define a code formula since the structural overstrength of a building is related to many factors, e.g. the bay width, the presence of irregularities in plan or elevation and the design PGA among others. Finally, it should be also noted that the presented study is limited to bare RC frame structures, without considering the influence of infill walls on the global dynamic behavior.

**Acknowledgments** This research study has been funded by Italian Department of Civil Protection in the framework of the national projects DPC-ReLUIS 2010–2013 and DPC-ReLUIS 2014 RS8. The authors acknowledge Eng. Maddalena Cimmino for the execution of numerical analyses and Raffaelina Divano, English language expert, for proofreading the paper.

## References

Ambraseys N, Smit P, Sigbjornsson R, Suhadolc P, Margaris B (2002) Internet-site for European strong-motion data. European Commission, Research-Directorate General, Environment and Climate Programme

American Society of Civil Engineers (2010) ASCE/SEI 7-10: minimum design loads for buildings and other structures. Reston, Virginia

Asteris PG, Cotsovos DM (2012) Numerical investigation of the effect of infill walls on the structural response of rc frames. Open Constr Build Technol J 6(SPEC. ISS. 1):164–181

Badillo-Almaraz H, Whittaker AS, Reinhorn AM (2007) Seismic fragility of suspended ceiling systems. Earthq Spectra 23(1):21–40. doi:10.1193/1.2357626

CEN (2004a) Eurocode 2: design of concrete structures—part 1-1: General rules and rules for buildings. EN 1992-1-1. Brussels, Belgium

CEN (2004b) Eurocode 8: design of structures for earthquake resistance—part 1: general rules, seismic actions and rules for buildings. EN 1998-1. Brussels, Belgium

Chaudhuri S, Villaverde R (2008) Effect of building nonlinearity on seismic response of nonstructural components: a parametric study. J Struct Eng 134(4):661–670. doi:10.1061/(ASCE)0733-9445(2008)134:4(661)

Chen Y, Soong TT (1988) Seismic response of secondary systems. Eng Struct 10(4):218–228. doi:10.1016/0141-0296(88)90043-0

Consiglio Superiore dei Lavori Pubblici (2009) Circolare 2 febbraio 2009, n. 617, Istruzioni per l'applicazione delle «Nuove norme tecniche per le costruzioni». G.U. n. 27 del 26-2-2009 (**in Italian**)

Council of Standards New Zealand (2004) Structural design actions part 5: earthquake actions—New Zealand—NZS 1170.5:2004. Standards New Zealand, Wellington, New Zealand

D'Ambrisi A, De Stefano M, Tanganelli M (2009) Use of pushover analysis for predicting seismic response of irregular buildings: a case study. J Earth Eng 13(8):1089–1100

Earthquake Engineering Research Institute (EERI) (1984) Nonstructural issues of seismic design and construction, publication 84-04. Berkeley, CA, USA

Fathali S, Lizundia B (2011) Evaluation of current seismic design equations for nonstructural components in tall buildings using strong motion records. Struct Design Tall Spec Build 20:30–46. doi:10.1002/tal.736

Fischinger M, Ercolino M, Kramar M, Petrone C, Isakovic T (2011) Inelastic seismic shear in multi-storey cantilever columns. Paper presented at the 3rd international conference on computational methods in structural dynamics and earthquake engineering, COMPDYN 2011, 25–28 May 2011. Corfu, Greece

Haselton CB (2006) Assessing seismic collapse safety of modern reinforced concrete moment frame buildings. Ph.D. thesis, Stanford University, CA, USA

Ibarra LF, Medina RA, Krawinkler H (2005) Hysteretic models that incorporate strength and stiffness deterioration. Earthq Eng Struct Dyn 34(12):1489–1511. doi:10.1002/eqe.495

International Conference of Building Officials (ICBO) (2000) AC 156 acceptance criteria for the seismic qualification of nonstructural components. ICBO Evaluation Service Inc, Whittier

Lin J, Mahin S (1985) Seismic response of light subsystems on inelastic structures. J Struct Eng 111(2):400–417. doi:10.1061/(ASCE)0733-9445(1985)111:2(400)

Lucchini A, Mollaioli F, Bazzurro P (2014) Floor response spectra for bare and infilled reinforced concrete frames. J Earth Eng 18(7):1060–1082. doi:10.1080/13632469.2014.916633

Maddaloni G, Magliulo G, Cosenza E (2012) Effect of the seismic input on non-linear response of R/C building structures. Adv Struct Eng 15(10):1861–1877

Magliulo G, Maddaloni G, Cosenza E (2007) Comparison between non-linear dynamic analysis performed according to EC8 and elastic and non-linear static analyses. Eng Struct 29(11):2893–2900. doi:10.1016/j.engstruct.2007.01.027

Magliulo G, Pentangelo V, Maddaloni G, Capozzi V, Petrone C, Lopez P, Talamonti R, Manfredi G (2012a) Shake table tests for seismic assessment of suspended continuous ceilings. Bull Earthq Eng 10(6):1819–1832. doi:10.1007/s10518-012-9383-6

Magliulo G, Petrone C, Capozzi V, Maddaloni G, Lopez P, Talamonti R, Manfredi G (2012b) Shake table tests on infill plasterboard partitions. Open Constr Build Technol J 6(Suppl 1-M10):155–163. doi:10.2174/1874836801206010155

Magliulo G, Ercolino M, Petrone C, Coppola O, Manfredi G (2014a) The emilia earthquake: the seismic performance of precast reinforced concrete buildings. Earthq Spectra 30(2):891–912. doi:10.1193/091012EQS285M

Magliulo G, Petrone C, Capozzi V, Maddaloni G, Lopez P, Manfredi G (2014b) Seismic performance evaluation of plasterboard partitions via shake table tests. Bull Earthq Eng 12(4):1657–1677. doi:10.1007/s10518-013-9567-8

Mander J, Priestley M, Park R (1988) Theoretical stress–strain model for confined concrete. J Struct Eng 114(8):1804–1826. doi:10.1061/(ASCE)0733-9445(1988)114:8(1804)

McKenna F, Fenves GL (2013) OpenSees manual. http://opensees.berkeley.edu. Pacific Earthquake Engineering Research Center, Berkeley, CA

Medina RA (2013) Seismic design horizontal accelerations for non-structural components. Paper presented at the Vienna congress on recent advances in earthquake engineering and structural dynamics 2013 (VEESD 2013), 28–30 August 2013, Vienna, Austria

Medina RA, Sankaranarayanan R, Kingston KM (2006) Floor response spectra for light components mounted on regular moment-resisting frame structures. Eng Struct 28(14):1927–1940. doi:10.1016/j.engstruct.2006.03.022

Menon A, Magenes G (2011) Definition of seismic input for out-of-plane response of masonry walls: II. Formulation. J Earth Eng 15(2):195–213. doi:10.1080/13632460903494446

Petrone C, Magliulo G, Manfredi G (2014) Shake table tests for the seismic assessment of hollow brick internal partitions. Eng Struct 72:203–214. doi:10.1016/j.engstruct.2014.04.044

Petrovčič S, Kilar V (2012) Effects of horizontal and vertical mass-asymmetric distributions on the seismic response of a high-rack steel structure. Adv Struct Eng 15(11):1977–1988. doi:10.1260/1369-4332.15.11.1977

Politopoulos I (2010) Floor spectra of MDOF nonlinear structures. J Earth Eng 14(5):726–742. doi:10.1080/13632460903427826

Ray-Chaudhuri S, Hutchinson TC (2011) Effect of nonlinearity of frame buildings on peak horizontal floor acceleration. J Earth Eng 15(1):124–142. doi:10.1080/13632461003668046

Rejec K, Isaković T, Fischinger M (2012) Seismic shear force magnification in RC cantilever structural walls, designed according to Eurocode 8. Bull Earthq Eng 10(2):567–586. doi:10.1007/s10518-011-9294-y

Rodriguez ME, Restrepo JI, Carr AJ (2002) Earthquake-induced floor horizontal accelerations in buildings. Earthq Eng Struct Dyn 31(3):693–718. doi:10.1002/eqe.149

Sankaranarayanan R, Medina RA (2007) Acceleration response modification factors for nonstructural components attached to inelastic moment-resisting frame structures. Earthq Eng Struct Dyn 36(14):2189–2210. doi:10.1002/eqe.724

Sewell RT, Cornell CA, Toro GR, McGuire RK (1988) A study of factors influencing floor response spectra in nonlinear multi-degree-of-freedom structures. Report no. 82. The John A. Blume Earthquake Engineering Center, Stanford University, Stanford, CA

Shome N, Cornell CA, Bazzurro P, Carballo JE (1998) Earthquakes, records, and nonlinear responses. Earthq Spectra 14(3):469–500. doi:10.1193/1.1586011

Singh M, Moreschi L, Suárez L, Matheu E (2006a) Seismic design forces. I: rigid nonstructural components. J Struct Eng 132(10):1524–1532. doi:10.1061/(ASCE)0733-9445(2006)132:10(1524)

Singh M, Moreschi L, Suárez L, Matheu E (2006b) Seismic design forces. II: flexible nonstructural components. J Struct Eng 132(10):1533–1542. doi:10.1061/(ASCE)0733-9445(2006)132:10(1533)

Taghavi S, Miranda E (2005) Approximate floor acceleration demands in multistory buildings. II: applications. J Struct Eng 131(2):212–220. doi:10.1061/(ASCE)0733-9445(2005)131:2(212)

Velasquez JF, Restrepo J, Blandon CA (2012) Floor rersponse spectra for the design of acceleration sensitive light nonstructural systems in buildings. Paper presented at the 15th world conference on earthquake engineering, 24–28 September 2013, Lisboa, Portugal

Villaverde R (1997) Seismic design of secondary structures: state of the art. J Struct Eng-Asce 123(8):1011–1019. doi:10.1061/(Asce)0733-9445(1997)123:8(1011)

Wieser J, Pekcan G, Zaghi AE, Itani A, Maragakis M (2013) Floor accelerations in yielding special moment resisting frame structures. Earthq Spectra 29(3):987–1002. doi:10.1193/1.4000167